JACS
JOURNAL OF THE AMERICAN CHEMICAL SOCIETY
Communication
pubs.acs.org/JACS

Cross-Linked Micellar Spherical Nucleic Acids from Thermoresponsive Templates

Resham J. Banga,[†,‡] Brian Meckes,[†,§] Suguna P. Narayan,[†,∥] Anthony J. Sprangers,[†,∥] SonBinh T. Nguyen,[*,†,§] and Chad A. Mirkin[*,†,§,‡]

[†]International Institute of Nanotechnology, [‡]Department of Chemical and Biological Engineering, [§]Department of Chemistry, and [∥]Department of Biomedical Engineering, Northwestern University, 2145 Sheridan Road, Evanston, Illinois 60208, United States

Supporting Information

ABSTRACT: A one-pot synthesis of micellar spherical nucleic acid (SNA) nanostructures using Pluronic F127 as a thermoresponsive template is reported. These novel constructs are synthesized in a chemically straightforward process that involves intercalation of the lipid tails of DNA amphiphiles (CpG motifs for TLR-9 stimulation) into the hydrophobic regions of Pluronic F127 micelles, followed by chemical cross-linking and subsequent removal of non-cross-linked structures. The dense nucleic acid shell of the resulting cross-linked micellar SNA enhances their stability in physiological media and facilitates their rapid cellular internalization, making them effective TLR-9 immunomodulatory agents. These constructs underscore the potential of SNAs in regulating immune response and address the relative lack of stability of noncovalent constructs.

Spherical nucleic acids (SNAs) have become an important platform for programmable assembly,[1] biodetection,[2,3] drug delivery,[4,5] and nucleic acid–based therapeutics.[6] Historically, SNAs have been synthesized by covalently immobilizing a dense layer of highly oriented nucleic acids onto a spherical gold nanoparticle core.[7] The resulting three-dimensional polyvalent architecture of the SNA makes it a higher affinity binder for complementary ligands than the linear sequence from which it is comprised.[8] The dense oligonucleotide shell of SNAs also enhances its resistance to enzymatic degradation,[9] thus increasing the overall lifetime of the oligonucleotide components. In addition, by engaging cell-surface receptors,[10] SNAs can actively traverse cell membranes without the need for transfection agents. As a result, SNAs have emerged as "single-entity" intracellular diagnostic tools,[2,11] gene-regulating structures,[6] and immunomodulatory agents[12] that exhibit minimal cytotoxicity and nonspecific immunogenic responses.[13]

Since the aforementioned physical and biological properties of SNAs are independent of the nature of the core,[8] a broad range of materials (Au,[7] Ag,[14] γ-Fe_2O_3,[15] CdSe,[16] Pt, Pd) have been used as templates for their syntheses.[8,16] However, concerns about the potential long-term toxicity and metabolic fate of metallic nanoparticle cores[17,18] have inspired a shift to the postsynthesis dissolution of the Au NP template[19] or the use of organic templates such as liposomes,[20] proteins,[21] and block copolymer nanostructures.[22,23] Arguably, an ideal SNA is one that can be rapidly made under mild conditions from biocompatible cores in size-tunable and monodisperse forms. As an amphiphilic block copolymer that is part of many FDA-approved drugs[24] and can be assembled into spherical micelles at room temperature at low critical micelle concentrations (CMC), Pluronic F127[25,26] ((poly(oxyethylene)-poly(oxypropylene)-poly(oxyethylene); PEO–PPO–PEO) is such an ideal SNA core material. In addition, since it has a thermoresponsive CMC, micelles made from Pluronic F127 can be easily assembled and disassembled based upon a change in temperature—as has been demonstrated for a wide range of hydrophobic cargos[27,28]—a property that can be extremely useful for purifying the targeted SNA architectures.[25,29]

Herein, we report a strategy that utilizes Pluronic F127-based micellar templates for the facile assembly of nucleic acids comprising hydrophobic lipid tails and stretches of T bases functionalized with C6-amines into sub-50 nm biocompatible SNA constructs (Scheme 1). The C6-amines can be subsequently cross-linked with PEGylated bis(sulfosuccinimidyl)suberate to increase the stability of the SNA. With this method, particles that are not fully cross-linked can be disassembled using the temperature-dependent properties of the Pluronic F127 block copolymer core. To demonstrate the versatility of this strategy, we have synthesized SNA constructs comprising 1826 and 7909 CpG DNA sequences that are known agonists for TLR9 and evaluated their structures,

Scheme 1. Assembly of Cross-Linked Micellar SNAs from Pluronic F127 Templates and Amphiphilic DNA

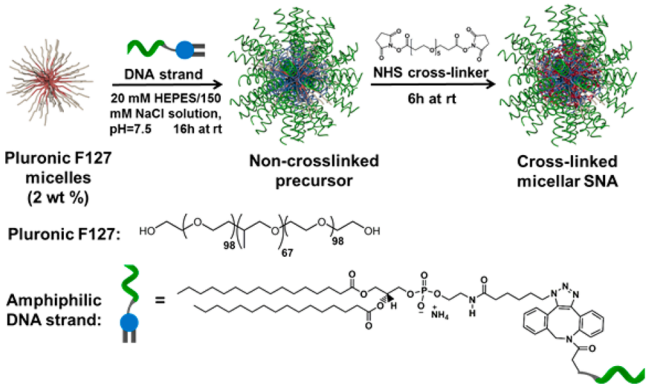

Received: December 29, 2016
Published: February 16, 2017

DOI: 10.1021/jacs.6b13359
J. Am. Chem. Soc. 2017, 139, 4278–4281

stabilities, and intracellular potencies with respect to TLR9 activation.[30]

Above their CMC of 1 wt %, Pluronic F127 block copolymers can assemble into small (~10 nm), monodisperse micelles that consist of a hydrophobic PPO core surrounded by a hydrophilic PEO shell.[31] In these size ranges, Pluronic F127-derived micelles have been shown to exhibit long *in vivo* circulation times and can deliver encapsulated chemotherapeutics into tumor tissues, presumably via the enhanced permeation and retention (EPR) effect.[32,33] For SNA assembly, we chose to synthesize micelles of 12 ± 2 nm diameter (PDI = 0.21 as measured by dynamic light scattering (DLS), ζ = −2 mV; 2 wt % dispersion of Pluronic F127) in 1× HEPES buffered saline (HBS). Surface functionalization of these micelles was readily achieved by the addition of an amphiphilic DNA (to a final concentration of ~10 μM; see Supporting Information (SI), Section S2 and Table S1), which comprises a hydrophobic lipid tail, a block of five amine-functionalized bases, and the desired nucleic acid sequence (20−25 base pairs), followed by equilibration overnight at room temperature prior to cross-linking. The hydrophobic DPPE lipid tail, attached covalently to the DNA via Cu-free click chemistry (see SI, Section S2), allows for surface immobilization of DNA onto the hydrophobic core of the micelles. In the final step, the nucleic acid strands were cross-linked at room temperature with a commercially available bis(succinimidyl)penta(ethylene glycol) ($BS(PEG)_5$) linker. *In situ* analysis of the reaction mixture shows particles with an increased size (25 ± 5 nm, PDI = 0.33) and a more negative surface charge (ζ = −15 mV), suggesting successful functionalization of the micelle core with the nucleic acid strands.

Since the CMC of Pluronic F127 is temperature-sensitive, isolation of the micellar SNAs from the excess Pluronic F127 and the non-cross-linked, unbound amphiphilic nucleic acids can be accomplished by low-temperature centrifugal filtration.[25] Indeed, lowering the temperature of the dispersion to 4 °C allows for the disassembly of any nonfunctionalized micelles (or those with low levels of functionalization) into individual polymer chains after cross-linking.[25] These left-over Pluronic-based components, together with unincorporated DNAs, can be removed via three low-temperature cycles of membrane-filter-centrifugation/resuspension (Figure 1B; see also SI, Section S2), which was verified with a standard colorimetric assay (see SI, Section S3).[25]

The purified micellar SNAs retain many of their as-synthesized particle characteristics (26 ± 2 nm, PDI = 0.34, ζ = −15 mV), confirming that the cross-linking was effective and the purification process did not cause a significant loss in the template-assembled DNA component (~60% DNA incorporation). Imaging of the purified micellar SNAs that have been deposited on a mica surface by atomic force microscopy (AFM, Figure 1C−D) showed spherical nanostructures (22 ± 8 nm) that are consistent with the addition of a shell of single-stranded DNA (~8 nm in length) onto the Pluronic F127 template. As synthesized, the average surface coverage of DNA strands on the micellar SNAs is ~150 ± 50 strands/particle, as determined by a combination of UV−vis spectroscopy (to determine total oligonucleotide content) and nanoparticle tracking analysis (to calculate the number of nanoparticles based upon dynamic light scattering and their Brownian motion) (see SI, Section S4).

The cooperative melting profiles of materials assembled from complementary SNAs are diagnostic indicators of the SNA structure.[8] This cooperative binding is a consequence of the

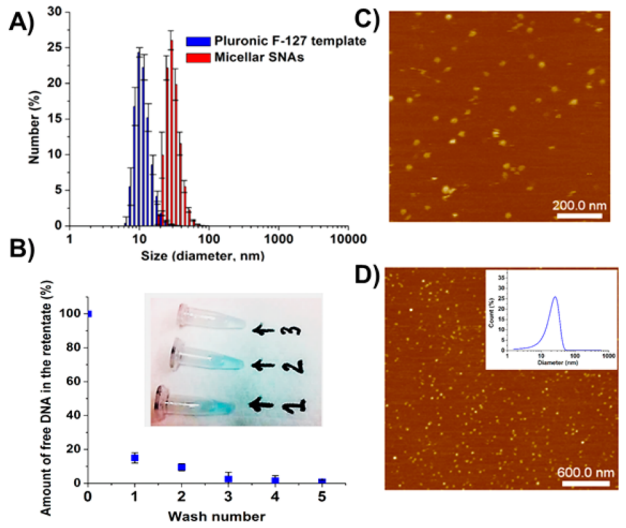

Figure 1. (A) DLS histograms of the Pluronic F127 templates before DNA insertion (blue) and the micellar SNAs after cross-linking (red). (B) Plot of the amount of free, unincorporated DNA in the solution (i.e., the dispersion of micellar SNAs), showing complete removal after three centrifugal washing steps at 4 °C. The inset is a photograph of the filtrates after the first three washes, showing that the blue color of the Cy-5 labeled DNA visually disappears after the third wash. (C−D) *In situ* AFM images of the micellar SNAs after being drop-cast on mica, showing the micellar SNAs as bright dots. The inset shows a distribution centering at 22 ± 8 nm, slightly smaller than the DLS data, as expected for embedded materials.

dense, uniform arrangement of nucleic acids on their surfaces, which allows them to hybridize in a polyvalent fashion. Indeed, when two samples of micellar SNAs with complementary nucleic acids were combined at room temperature, visually observable aggregates were formed that exhibited a substantial increase in melting temperature (71.5 vs 55 °C for the free DNA duplex at fixed total DNA and salt concentrations, Figure 2B) along with a narrow melting transition (full-width at half-maximum ~2 °C; Figure 2B).[7]

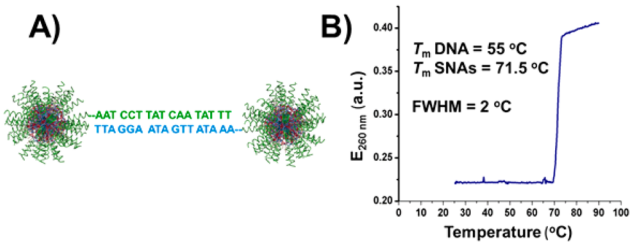

Figure 2. (A) A schematic representation of the hybridization of micellar SNAs with complementary SNAs. (B) Melting profile of micellar SNA conjugates that have hybridized to the complementary nanoconstructs (SI, Section S5). The hybridized micellar SNAs exhibit a sharper melting transition with a higher melting point in comparison to the corresponding hybridized duplex between complementary linear nucleic acids.

The micellar SNAs exhibit remarkable stability in biological media at physiological conditions. DNA dissociation and interparticle fusion were not observed after 7 days of storage at 37 °C, as analyzed by gel electrophoresis (see SI, Figure S5). This enhanced thermal stability can be attributed to the electrostatic repulsive forces of the negatively charged DNA strands on the particle surface.[20,34] This DNA corona, which is

DOI: 10.1021/jacs.6b13359
J. Am. Chem. Soc. 2017, 139, 4278−4281

common to SNAs, is hypothesized to decrease the propensity of SNAs to be degraded by nucleases,[9] and cross-linking of the nucleic acids should further enhance the serum stability and lifetime of the SNAs. This was confirmed by a fluorescence "turn-on" experiment based on an SNA comprising a $DilC_{18}$ dye-encapsulated Pluronic F127 core and a blackhole quencher (BHQ)-modified DNA shell (Figure 3A; also see SI, Section

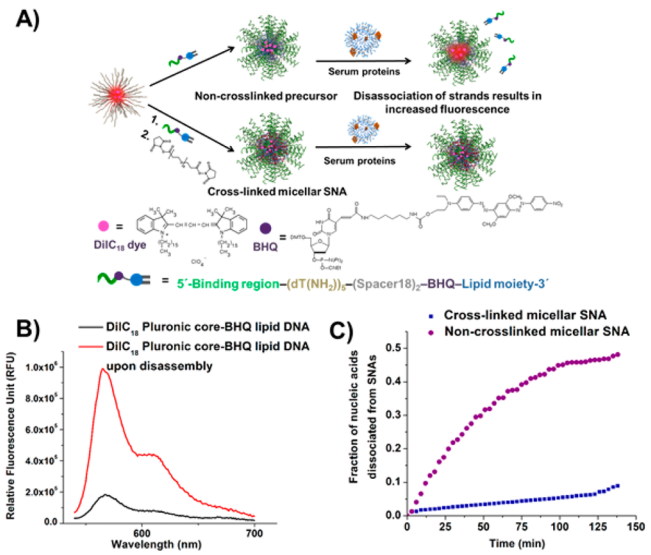

Figure 3. (A) A schematic representation of the serum-stability study of cross-linked micellar SNAs. In the non-cross-linked precursor (top branch), dissociation of the BHQ-modified DNA would result in increased $DilC_{18}$ fluorescence compared to the cross-linked analog (bottom branch). (B) The fluorescent profiles of $DilC_{18}$-encapsulated micelles that was functionalized with the BHQ-T_{20}-lipid material but not cross-linked (i.e., the non-cross-linked precursor to the micellar SNA), before (black trace) and after (red trace) dissociation of DNA from the micelle template, showing an increase in fluorescence upon disassembly. (C) The fluorescent profiles of the cross-linked micellar SNAs and the non-cross-linked precursor after being incubated at 37 °C in 10% serum-containing media, showing stark contrast in stability. Unlike their non-cross-linked precursors, the cross-linked micellar SNAs show minimal dissociation.

S8). Dissociation of the lipid-tailed DNA from the dye-labeled core should result in an increase in fluorescence and provide a measure of stability (Figure 3B). Indeed, incubation of the $DilC_{18}$-encapsulated, BHQ-modified micellar SNAs in 10% serum media shows minimal increase in fluorescence over a period of 2 h, suggesting that the structures are quite stable in serum. In contrast, incubating the non-cross-linked precursor in the same 10% serum media resulted in a significant increase in fluorescence due to the dissociation of the intercalated DNA strands from the $DilC_{18}$-encapsulated Pluronic F127 core (Figure 3C).

As expected, the nucleic acid shell on the surface of the micellar SNAs also facilitates their rapid cellular uptake into macrophages.[12] Indeed, exposing HEK-Blue mTLR9 cells to micellar SNAs comprising Cy5-labeled DNA for 4 h resulted in significant cellular uptake in comparison to free Cy5-labeled DNA (Figure 4A) as evaluated by confocal microscopy and flow cytometry (Figure 4B). Consistent with the complete biocompatibility of its design, our micellar SNAs did not exhibit any cytotoxicity (Figure 4C), even at higher DNA concentrations, where delivery using traditional cationic transfection

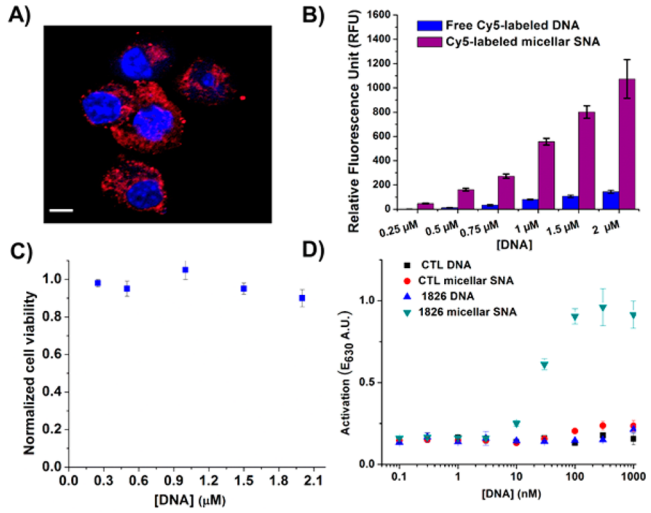

Figure 4. (A) A confocal fluorescent micrograph of HEK-Blue mTLR9 cells that were incubated with Cy5-labeled micellar SNAs ([DNA] = 100 nM) for 4 h. Cell nuclei were stained with Hoechst 33342 (scale bar = 20 μm). (B) Flow cytometry analysis of HEK-Blue mTLR9 cells that have been incubated with free Cy5-labeled DNA (blue bars) and Cy5-labeled micellar SNAs after 16 h (purple bars), showing a higher fluorescence intensity for the latter. (C) A cell-viability assay for HEK-Blue mTLR9 cells after treatment with micellar SNAs for 24 h. (D) Plots of the amounts of secreted alkaline phosphatase (SEAP) by HEK-Blue cells, as visualized by a colorimetric assay, showing enhanced immunostimulatory activity by micellar SNAs in comparison to control micellar SNAs bearing a T_{20} sequence and unmodified linear nucleic acids.

agents such as Dharmafect can cause detrimental changes in cellular morphology[35] and eventual cell death.[20]

The ability of SNAs to independently enter cells at high concentrations via endocytosis[10] has made them a promising therapeutic platform.[12,36] As an example, SNAs comprising immunostimulatory (IS) nucleic acids were recently shown to accumulate in endosomes at early time points, resulting in enhanced TLR9 activation, a key requirement for producing an immunostimulatory response.[12] To this end, we investigated the TLR9 immunomodulatory activity of cross-linked micellar SNAs comprising 1826[37] and 7909[38] CpG motifs, known mTLR9 agonists, in HEK- and Ramos-Blue cells, respectively. As hypothesized, we observed a dose-dependent immunostimulatory response for the micellar SNAs in both cell types in contrast to the untreated and negative controls (Figure 4D; see also SI, Figure S8). Importantly, the cross-linked micellar SNAs perform markedly better than linear unmodified strands where no activity was observed even at total DNA concentrations that are orders of magnitude higher than that in the SNAs.

In conclusion, this work has introduced a new and promising class of cross-linked micellar SNAs that show strong potential for therapeutic development. The ease in which this novel SNA can be synthesized and purified using a thermoresponsive template, their extended stability, and their enhanced intracellular activity all point to their potential for impacting gene regulation and immune therapy applications across a wide variety of indications.

■ ASSOCIATED CONTENT

Supporting Information

The Supporting Information is available free of charge on the ACS Publications website at DOI: 10.1021/jacs.6b13359.

DOI: 10.1021/jacs.6b13359
J. Am. Chem. Soc. 2017, 139, 4278−4281

General material and instrumentation information; synthesis procedures; characterization data; stability data; additional figures (PDF)

AUTHOR INFORMATION

Corresponding Authors

*E-mail: stn@northwestern.edu.
*E-mail: chadnano@northwestern.edu.

ORCID

SonBinh T. Nguyen: 0000-0002-6977-3445
Chad A. Mirkin: 0000-0002-6634-7627

Notes

The authors declare no competing financial interest.

ACKNOWLEDGMENTS

This material is based upon work supported by the Air Force Office of Scientific Research (FA9550-12-1-0141), the National Cancer Institute of the NIH (U54CA199091), and the NTU-NU Institute for NanoMedicine located at the International Institute for Nanotechnology (IIN), Northwestern University (NU), USA and the Nanyang Technological University (NTU), Singapore. B.M., S.P.N., and A.J.S acknowledge an IIN fellowship, an NDSEG fellowship, and an NSF GRF, respectively. This work made use of the MALDI-ToF equipment (purchased with support from Northwestern University and the State of Illinois) at the NU Integrated Molecular Structure Education and Research Center (IMSERC) and the NanoSight instrument (purchased with support from the IIN) at the NU Keck Biophysics Facility.

REFERENCES

(1) Macfarlane, R. J.; Lee, B.; Jones, M. R.; Harris, N.; Schatz, G. C.; Mirkin, C. A. *Science* **2011**, *334*, 204−208.
(2) Seferos, D. S.; Giljohann, D. A.; Hill, H. D.; Prigodich, A. E.; Mirkin, C. A. *J. Am. Chem. Soc.* **2007**, *129*, 15477−15479.
(3) Sun, W.; Lu, Y.; Mao, J.; Chang, N.; Yang, J.; Liu, Y. *Anal. Chem.* **2015**, *87*, 3354−3359.
(4) Tan, X.; Li, B. B.; Lu, X.; Jia, F.; Santori, C.; Menon, P.; Li, H.; Zhang, B.; Zhao, J. J.; Zhang, K. *J. Am. Chem. Soc.* **2015**, *137*, 6112−6115.
(5) Tan, X. Y.; Lu, X. G.; Jia, F.; Liu, X. F.; Sun, Y. H.; Logan, J. K.; Zhang, K. *J. Am. Chem. Soc.* **2016**, *138*, 10834−10837.
(6) Rosi, N. L.; Giljohann, D. A.; Thaxton, C. S.; Lytton-Jean, A. K.; Han, M. S.; Mirkin, C. A. *Science* **2006**, *312*, 1027−1030.
(7) Mirkin, C. A.; Letsinger, R. L.; Mucic, R. C.; Storhoff, J. J. *Nature* **1996**, *382*, 607−609.
(8) Cutler, J. I.; Auyeung, E.; Mirkin, C. A. *J. Am. Chem. Soc.* **2012**, *134*, 1376−1391.
(9) Chung, C. H.; Kim, J. H.; Jung, J.; Chung, B. H. *Biosens. Bioelectron.* **2013**, *41*, 827−832.
(10) Choi, C. H.; Hao, L.; Narayan, S. P.; Auyeung, E.; Mirkin, C. A. *Proc. Natl. Acad. Sci. U. S. A.* **2013**, *110*, 7625−7630.
(11) Wang, Y. Y.; Wu, C. C.; Chen, T.; Sun, H.; Cansiz, S.; Zhang, L. Q.; Cui, C.; Hou, W. J.; Wu, Y.; Wan, S.; Cai, R.; Liu, Y.; Sumerlin, B. S.; Zhang, X. B.; Tan, W. H. *Chem. Sci.* **2016**, *7*, 6041−6049.
(12) Radovic-Moreno, A. F.; Chernyak, N.; Mader, C. C.; Nallagatla, S.; Kang, R. S.; Hao, L.; Walker, D. A.; Halo, T. L.; Merkel, T. J.; Rische, C. H.; Anantatmula, S.; Burkhart, M.; Mirkin, C. A.; Gryaznov, S. M. *Proc. Natl. Acad. Sci. U. S. A.* **2015**, *112*, 3892−3897.
(13) Massich, M. D.; Giljohann, D. A.; Schmucker, A. L.; Patel, P. C.; Mirkin, C. A. *ACS Nano* **2010**, *4*, 5641−5646.
(14) Lee, J. S.; Lytton-Jean, A. K.; Hurst, S. J.; Mirkin, C. A. *Nano Lett.* **2007**, *7*, 2112−2115.
(15) Cutler, J. I.; Zheng, D.; Xu, X.; Giljohann, D. A.; Mirkin, C. A. *Nano Lett.* **2010**, *10*, 1477−1480.
(16) Zhang, C.; Macfarlane, R. J.; Young, K. L.; Choi, C. H. J.; Hao, L.; Auyeung, E.; Liu, G.; Zhou, X.; Mirkin, C. A. *Nat. Mater.* **2013**, *12*, 741−746.
(17) Alkilany, A. M.; Murphy, C. J. *J. Nanopart. Res.* **2010**, *12*, 2313−2333.
(18) Arnida; Malugin, A.; Ghandehari, H. *J. Appl. Toxicol.* **2010**, *30*, 212−217.
(19) Cutler, J. I.; Zhang, K.; Zheng, D.; Auyeung, E.; Prigodich, A. E.; Mirkin, C. A. *J. Am. Chem. Soc.* **2011**, *133*, 9254−9257.
(20) Banga, R. J.; Chernyak, N.; Narayan, S. P.; Nguyen, S. T.; Mirkin, C. A. *J. Am. Chem. Soc.* **2014**, *136*, 9866−9869.
(21) Brodin, J. D.; Auyeung, E.; Mirkin, C. A. *Proc. Natl. Acad. Sci. U. S. A.* **2015**, *112*, 4564−4569.
(22) Watson, K. J.; Park, S. J.; Im, J. H.; Nguyen, S. T.; Mirkin, C. A. *J. Am. Chem. Soc.* **2001**, *123*, 5592−5593.
(23) Li, Z.; Zhang, Y.; Fullhart, P.; Mirkin, C. A. *Nano Lett.* **2004**, *4*, 1055−1058.
(24) Diniz, I. M. A.; Chen, C.; Xu, X. T.; Ansari, S.; Zadeh, H. H.; Marques, M. M.; Shi, S. T.; Moshaverinia, A. *J. Mater. Sci.: Mater. Med.* **2015**, *26*, 153.
(25) Zhang, Y.; Jeon, M.; Rich, L. J.; Hong, H.; Geng, J.; Zhang, Y.; Shi, S.; Barnhart, T. E.; Alexandridis, P.; Huizinga, J. D.; Seshadri, M.; Cai, W.; Kim, C.; Lovell, J. F. *Nat. Nanotechnol.* **2014**, *9*, 631−638.
(26) Batrakova, E. V.; Kabanov, A. V. *J. Controlled Release* **2008**, *130*, 98−106.
(27) Zhang, Y.; Song, W.; Geng, J.; Chitgupi, U.; Unsal, H.; Federizon, J.; Rzayev, J.; Sukumaran, D. K.; Alexandridis, P.; Lovell, J. F. *Nat. Commun.* **2016**, *7*, 11649.
(28) Zhang, Y.; Wang, D.; Goel, S.; Sun, B.; Chitgupi, U.; Geng, J.; Sun, H.; Barnhart, T. E.; Cai, W.; Xia, J.; Lovell, J. F. *Adv. Mater.* **2016**, *28*, 8524−8530.
(29) Linse, P.; Malmsten, M. *Macromolecules* **1992**, *25*, 5434−5439.
(30) Krieg, A. M. *Nat. Rev. Drug Discovery* **2006**, *5*, 471−484.
(31) Lin, Y. N.; Alexandridis, P. *J. Phys. Chem. B* **2002**, *106*, 10834−10844.
(32) Liu, L. W.; Yong, K. T.; Roy, I.; Law, W. C.; Ye, L.; Liu, J. W.; Liu, J.; Kumar, R.; Zhang, X. H.; Prasad, P. N. *Theranostics* **2012**, *2*, 705−713.
(33) Greish, K. In *Cancer Nanotechnology*; Grobmyer, S. R., Moudgil, B. M., Eds.; Humana Press: New York, NY, 2010; pp 25−37.
(34) Seferos, D. S.; Prigodich, A. E.; Giljohann, D. A.; Patel, P. C.; Mirkin, C. A. *Nano Lett.* **2009**, *9*, 308−311.
(35) Antczak, C.; Mahida, J. P.; Singh, C.; Calder, P. A.; Djaballah, H. *Comb. Chem. High Throughput Screening* **2014**, *17*, 12−24.
(36) Jensen, S. A.; Day, E. S.; Ko, C. H.; Hurley, L. A.; Luciano, J. P.; Kouri, F. M.; Merkel, T. J.; Luthi, A. J.; Patel, P. C.; Cutler, J. I.; Daniel, W. L.; Scott, A. W.; Rotz, M. W.; Meade, T. J.; Giljohann, D. A.; Mirkin, C. A.; Stegh, A. H. *Sci. Transl. Med.* **2013**, *5*, 209ra152−11.
(37) Ramirez-Ortiz, Z. G.; Specht, C. A.; Wang, J. P.; Lee, C. K.; Bartholomeu, D. C.; Gazzinelli, R. T.; Levitz, S. M. *Infect. Immun.* **2008**, *76*, 2123−2129.
(38) Cooper, C. L.; Davis, H. L.; Morris, M. L.; Efler, S. M.; Al Adhami, M.; Krieg, A. M.; Cameron, D. W.; Heathcote, J. *J. Clin. Immunol.* **2004**, *24*, 693−701.

DOI: 10.1021/jacs.6b13359
J. Am. Chem. Soc. 2017, 139, 4278−4281